6472–6481 *Nucleic Acids Research, 2008, Vol. 36, No. 20* *Published online 14 October 2008*
doi:10.1093/nar/gkn667

Translation affects YoeB and MazF messenger RNA interferase activities by different mechanisms

Mikkel Christensen-Dalsgaard[1,2] and Kenn Gerdes[1,*]

[1]Institute for Cell and Molecular Biosciences, Medical School, Newcastle University, Newcastle, NE2 4HH, UK and [2]Department of Biochemistry & Molecular Biology, University of Southern Denmark, Campusvej 55, DK-5230 Odense M, Denmark

Received May 27, 2008; Revised July 16, 2008; Accepted September 22, 2008

ABSTRACT

Prokaryotic toxin–antitoxin loci encode mRNA cleaving enzymes that inhibit translation. Two types are known: those that cleave mRNA codons at the ribosomal A site and those that cleave any RNA site specifically. RelE of *Escherichia coli* cleaves mRNA at the ribosomal A site *in vivo* and *in vitro* but does not cleave pure RNA *in vitro*. RelE exhibits an incomplete RNase fold that may explain why RelE requires its substrate mRNA to presented by the ribosome. In contrast, RelE homologue YoeB has a complete RNase fold and cleaves RNA independently of ribosomes *in vitro*. Here, we show that YoeB cleavage of mRNA is strictly dependent on translation of the mRNA *in vivo*. Non-translated model mRNAs were not cleaved whereas the corresponding wild-type mRNAs were cleaved efficiently. Model mRNAs carrying frameshift mutations exhibited a YoeB-mediated cleavage pattern consistent with the reading frameshift thus giving strong evidence that YoeB cleavage specificity was determined by the translational reading frame. In contrast, site-specific mRNA cleavage by MazF occurred independently of translation. In one case, translation seriously influenced MazF cleavage efficiency, thus solving a previous apparent paradox. We propose that translation enhances MazF-mediated cleavage of mRNA by destabilization of the mRNA secondary structure.

INTRODUCTION

Toxin–antitoxin (TA) loci encode two components, a 'toxin' whose ectopic overproduction inhibits translation or replication and an antitoxin that inhibits the toxin by direct protein–protein contact (1,2). Prokaryotic chromosomes encode a plethora of TA loci that have been grouped into seven independent families based on toxin sequence similarities. Some slowly growing and free-living organisms have particularly many TA loci while obligatory intracellular organisms have few or none. For example, *Mycobacterium tuberculosis* has more than 60 TA loci, while *M. leprae* has retained two TA pseudo-loci only (3). These observations are consistent with the proposal that the TA loci function as stress response elements (1,4–11).

The molecular targets of the toxins have been of particular interest. Four independent toxin families that inhibit translation are known (RelE, MazF, HicA and Doc). Doc of prophage P1 inhibits translation by interacting with the ribosomal S30 subunit but probably does not cleave RNA (12). Members of the three other toxin families, RelE, MazF and HicA, are mRNA Interferases (mIs) that inhibit translation by mRNA cleavage (13,14) (Jørgensen *et al.*, submitted for publication). RelE was the first mI to be discovered. RelE cleaved mRNA positioned at the ribosomal A site, between the second and the third base of the A site codon, both *in vitro* (13) and *in vivo* (15). RelE did not cleave naked RNA *in vitro* and did not cleave mRNA outside their coding regions *in vivo*. Interestingly, archaeal RelE homologues distantly related to RelE of *Escherichia coli* cleaved mRNA positioned at the A site in a pattern very similar to that of RelE (15).

Many RelE homologues have been identified in Bacteria and Archaea (1,6,16). Thus, in a recent bioinformatics survey, we identified 400 relBE loci in ≈200 prokaryotic genomes. The RelE family of proteins is highly diverse with very few conserved amino acids. Nevertheless, sequence comparisons and structural analyses together have shown that the members of the mI families HigB, YoeB, YafQ and YhaV all belong to the RelE superfamily (17–21). The crystal structure of YoeB of *E. coli* revealed a microbial RNase fold and sequence alignment suggested that RelE has a similar RNAse fold (21). The same study also showed that, in contrast to RelE, YoeB can cleave naked RNA *in vitro*. This difference was suggested to be explained by the fact that RelE lacks several amino acids

*To whom correspondence should be addressed. Tel: +44 191 222 5318; Fax: +44 191 222 7424; Email: kenn.gerdes@ncl.ac.uk

predicted to be essential for catalytic activity. RelE's lack of catalytic activity *in vitro* may reflect that RelE requires that the substrate is presented at the ribosomal A site.

MazF of *E. coli* is another well-characterized mI. MazF cleaves RNA substrates at ACA sites both *in vivo* and *in vitro* (14,22). MazF and MazF homologues cleave RNA preferentially at single-stranded regions (23,24) although cleavages at sites presumed to be in a double-stranded configuration have also been observed (25,26). However, we observed that MazF cleavage of one model substrate *in vivo* depended on translation (5).

The specific biological function of mIs are known in a few cases only (4,27) and it is thus important to understand, in depth, their substrate specificities. Here, we describe a method that is generally useful for the analysis of mI activity *in vivo*. We employ the method to analyse the activities of YoeB and MazF and compare them with two other well-characterized mIs, RelE and HigB. We find that the cleavage specificity of all three RelE homologues (RelE and YoeB of *E. coli*; K-12 and HigB-1 of *Vibrio cholerae*) depend strictly on translation of the substrate RNA. In contrast, MazF cleavage specificity does not depend on substrate translation. However, the efficiency of MazF cleavage was with one model substrate highly stimulated by translation. Our results show that translation affect different mIs by different molecular mechanisms.

MATERIALS AND METHODS

Strains and plasmids used and constructed in this work are listed in Table 1. DNA oligonucleotides are listed in Table 2.

Table 1. Strains and plasmids

Strains/plasmids	Genotype/plasmid properties	References
MG1655	Wild-type *E. coli* K-12	
MG1655Δ*lpp*	Δ*lpp*	(15)
MG1655Δ*dksA*	Δ*dksA*	Jørgensen,M.G., unpublished data
Plasmids		
pBAD33	p15; *cat araC* pBAD	(29)
pOU254	R1; *bla par mcs-lacZYA*	Jensen,R.B., unpublished data
pMCD3	pBAD33; pBAD::*higB-1*	(18)
pMCD3326	pBAD33; BAD::SD_{opt}::*mazF*	This work
pMG3323	pBAD33; pBAD::*relE*	(15)
pRB100	pBAD33; BAD::SD_{opt}::*yoeB*	Ramisetty,B.C.M., unpublished data
pKW254T	R1; terminator from pMG25	Winther, K, unpublished
pMCD25410	R1; pKW254T *lpp*	This work
pMCD25411	R1; pKW254T *lpp″*	This work
pMCD25412	R1; pKW254T *lpp′*	This work
pMCD25420	R1; pKW254T *dksA*	This work
pMCD25421	R1; pKW254T *dksA″*	This work
pMCD25422	R1; pKW254T *dksA′*	This work
pSC710	R1; *bla par lpp*	(15)
pSC711	R1; *bla par lpp* ATG1AAG	(15)
pSC320	pBR322, *tet*, *ssrA* and *smpB*	(15)
pSC321	pBR322, *tet*, *ssrA″* and *smpB*	(15)
pSC333	pUC; pGEM3, *bla*, T_7::*lpp*	(15)

Northern blotting analysis

Cells were grown in LB medium at 37°C. At an OD_{450} of 0.5, the cultures were diluted 10 times and grown to an OD of 0.5 and transcription of the mI gene was induced by the addition of 0.2% arabinose. To inhibit translation, chloramphenicol (50 μg/ml) was added. For northern blotting analysis, total RNA was fractionated by PAGE (6% low bis acrylamide), blotted to a Zeta probe nylon membrane and hybridized with a single-stranded ^{32}P-labbelled riboprobe complementary to the RNA of interest. For *lpp* mRNA hybridization, the radioactive probe was generated by T7 RNA polymerase using linearized plasmid DNA of pSC333 as the template. The riboprope used to detect *dksA* mRNA was transcribed from a PCR fragment containing the partial *dksA* gene and the T7 promoter (constructed using the primers *dksA* probe-f and *dksA* T7 probe-r).

Primer extension analysis

Semi-quantitative primer extension analysis was performed essentially as described previously (28). The stop codons of mRNAs originating from pKW254T derivatives were

Table 2. DNA oligonucleotides used

Oligonucleotide name	Sequence
mazF-SalI-SD-up	5′-CCCCCGTCGACTCAAGGAGTTTTA TAAATGGTAAGCCGATACGTACCC
mazF-HindIII-down	5′-CCCCCAAGCTTTAACACTACCCAA TCAGTACG
TRANSTERM#CCW	5′-CCCCGAATTCGATTCAACCCCTTC TTCGATC
term-bamH1-kpnI-sacI-pmlI-xhoI#CW	5′-CCCCCGGATCCGGTACCGAGCTCC ACGTG CTCGAG-GCCAAGCTTAAT TAGCTGAGC
lpp-BamHI-sacI#CW	5′-CCCCCGGATCCGAGCTCGGAAGCA TCCTGTTTTCTCTC
lpp-pmlII-xhoI#CCW	5′-CCCCCCACGTGCTCGAGGTACTAT TACTTGCGGTATTTAG
lpp 1AAG-1	5′-GAGGGTATTAATAAAGAAAGCTA CTAAAC
lpp 1AAG-2	5′-GTTTAGTAGCTTTCTTTATTAATA CCCTC
lpp 6ACT-cw	5′ATGAAAGCTACTAAAACTGGTACT GGGCGCGG
lpp 6ACT-ccw	5′CCGCGCCCAGTACCAGTTTTAGTA GCTTTCAT
dksA-bamH1-sacI#CW	5′- CCCCCGGATCCGAGCTCGTCGCG TGCGCAAATACGC
dksA-pmlI-xhoI#CCW	5′- CCCCCCACGTGCTCGAGGGCTGT AATTAGCCAGCCATC
dksA 1AAG-cw	5′-GTTAAGGAGAAGCAACAAGCAAG AAGGGCAAAAC
dksA 1AAG-ccw	5′-GTTTTGCCCTTCTTGCTTGTTGCTT CTCCTTAAC
dksA 2CAA-cw	5′-GGAGAAGCAACATGCAAAGAAGG GCAAAACCG
dksA 2CAA-ccw	5′-CGGTTTTGCCCTTCTTTGCATGTT GCTTCTCC
lpp 26	5′-CAGCTGGTCAACTTTAGCGTTC AGAG
dksA PE1	5′-GATATGGTTCCACCCCAGCG
pKW71D-3#PE	5′-GAGGTCATTACTGGATCTATCAAC
10SA-2	5′-GCCCCTCGGCATGCACC
dksA probe– f	5′-CAACTTCCCGGACCCGGTAG
dksA T7 probe- r	5′-GGGCCTAATACGACTCACTATA GGGGATGCACAGATCGGCTGTCG

mapped with the primer pKW71D-3#PE, which is complementary to the linker RNA of pKW254T. The primer *lpp* 21 was used to map the 5′-end of *lpp* RNA. The 5′-end of *dksA* mRNA was mapped using the primer *dksA* PE1.

Plasmids constructed

pMCD3326. The *mazF* gene was amplified from chromosomal DNA of MG1655 with primers *mazF*-SalI-SD-up and *mazF*-HindIII-down. The PCR product was digested with SalI and HindIII and inserted into pBAD33. The resulting plasmid contains the *mazF* gene with an efficient SD sequence (from *parM* of plasmid R1) downstream of the P_{BAD} promoter.

pRB100. A KpnI-XmnI DNA fragment of pKP3059 carrying the *E. coli yoeB* gene was inserted into pBAD33 cleaved with KpnI and HindII.

pKW254T. The region of pMG25 containing the $rrnB_{t1}$ $rrnB_{t2}$ transcriptional terminators and ≈100-bp upstream was amplified using primers TRANSTERM#CCW and term-bamH1-kpnI-sacI-pmlI-xhoI#CW. The PCR product was digested with EcoRI and BamHI and inserted into pOU254.

pMCD25410. The *lpp* gene of MG1655 was amplified from chromosomal DNA using the primers *lpp*-BamH1-sacI#CW and *lpp*-pmlI-xhoI-#CCW. The PCR fragment was digested with BamHI and XhoI and inserted into pKW254T. The plasmid therefore expresses an *lpp* mRNA with an additional 100-bp linker RNA downstream of the stop codon.

pMCD25411. The *lpp* gene of MG1655 was amplified with primers *lpp*-BamH1-sacI#CW and *lpp* 1AAG-2 in addition to *lpp* 1AAG-1 and *lpp*-pmlI-xhoI-#CCW. The two overlapping PCR products were used as templates in a second round of PCR using the primers *lpp*-BamH1-sacI#CW and *lpp*-pmlI-xhoI-#CCW. The resulting PCR product was digested with BamHI and XhoI and inserted into pKW254T. The plasmid encodes a non-translatable *lpp* gene (AAG replaces the natural start codon).

pMCD25412. The *lpp* gene of MG1655 was amplified with primers *lpp*-BamH1-sacI#CW and *lpp* 6ACT-ccw in addition to *lpp* 6ACT-cw and *lpp*-pmlI-xhoI-#CCW. The two overlapping PCR products were used as templates in a second round of PCR using primers *lpp*-BamH1-sacI#CW and *lpp*-pmlI-xhoI-#CCW. The resulting PCR product was digested with BamHI and XhoI and inserted into pKW254T. The plasmid encodes an *lpp* gene with an extra A inserted between the fifth and the sixth codon, thus generating a frameshift in *lpp*.

pMCD25420. The *dksA* gene of MG1655 was amplified with primers *dksA*-bamH1-sacI#CW and *dksA*-pmlI-xhoI#CCW. The PCR fragment was digested with BamHI and XhoI and inserted into pKW254T. The plasmid encodes *dksA* with an additional 100-bp linker RNA downstream of the stop codon.

pMCD25421. The *dksA* gene of MG1655 was amplified with primers *dksA*-bamH1-sacI#CW and *dksA* 1AAG-ccw in addition to *dksA* 1AAG-cw and *dksA*-pmlI-xhoI#CCW. The two overlapping PCR products were used as templates in a second round of PCR using primers *dksA*-bamH1-sacI#CW and *dksA*-pmlI-xhoI#CCW. The resulting PCR product was digested with BamHI and XhoI and inserted into pKW254T. The plasmid encodes a non-translatable *dksA* gene (AAG replaces the natural start codon).

pMCD25422. The *dksA* gene of MG1655 was amplified with primers *dksA*-bamH1-sacI#CW and *dksA* 2CAA-ccw in addition to *dksA* 2CAA-cw and *dksA*-pmlI-xhoI#CCW. The two overlapping PCR products were used as templates in a second round of PCR using primers *dksA*-bamH1-sacI#CW and *dksA*-pmlI-xhoI#CCW. The resulting PCR product was digested with BamHI and XhoI and inserted into pKW254T. The plasmid encodes a *dksA* messenger with an extra A inserted in the second codon, thus creating a reading frameshift.

RESULTS

Development of a novel strategy to analyse mI activity

We found it advantageous to generate plasmids that express model RNAs suitable for the analysis of mI activity *in vivo*. Such plasmid derivatives have two advantages: first, the RNA can be expressed at increased levels as compared to the chromosome-encoded RNA, thereby increasing the resolution and sensitivity of the analysis. Second, specific mutations are easily introduced into plasmid-encoded test genes. When we analysed a model RNA expressed from a plasmid, the corresponding chromosomal gene was deleted thus to avoid interfering signals from the endogenous mRNA. We employed two model mRNAs, *lpp* and *dksA*, both of which encode non-essential proteins. DNA fragments encoding the wild-type *lpp* and *dksA* genes and their native promoters were inserted into pKW254T, a plasmid that carries an efficient primer annealing site adjacent to a multiple cloning region (Figure 1A), thereby resulting in pMCD25410 and pMCD25420 (Figure 1B and C). Plasmids pMCD25411 and pMCD25421 carry point mutations in the start codons of *lpp* and *dksA* reading frames, respectively, thereby preventing translation of the reading frames. In plasmid pMCD25412, an A base was inserted between the fifth and sixth codons of *lpp*. This frameshift mutation generates a novel small reading frame that terminates prematurely as indicated in the figure. Similarly, in pMCD25422, an A base was inserted between the second and third codons of *dksA* that also in this case generates a novel small reading frame that stops prematurely.

YoeB activity depends on translation

The *relE* and *yoeB* genes of *E. coli*, K-12 and the *higB-1* gene of *V. cholerae* were inserted into plasmid pBAD33 that carries an arabinose-inducible promoter. Next, the mI production plasmids were transformed into strains MG1655Δlpp and MG1655ΔdksA carrying the reporter

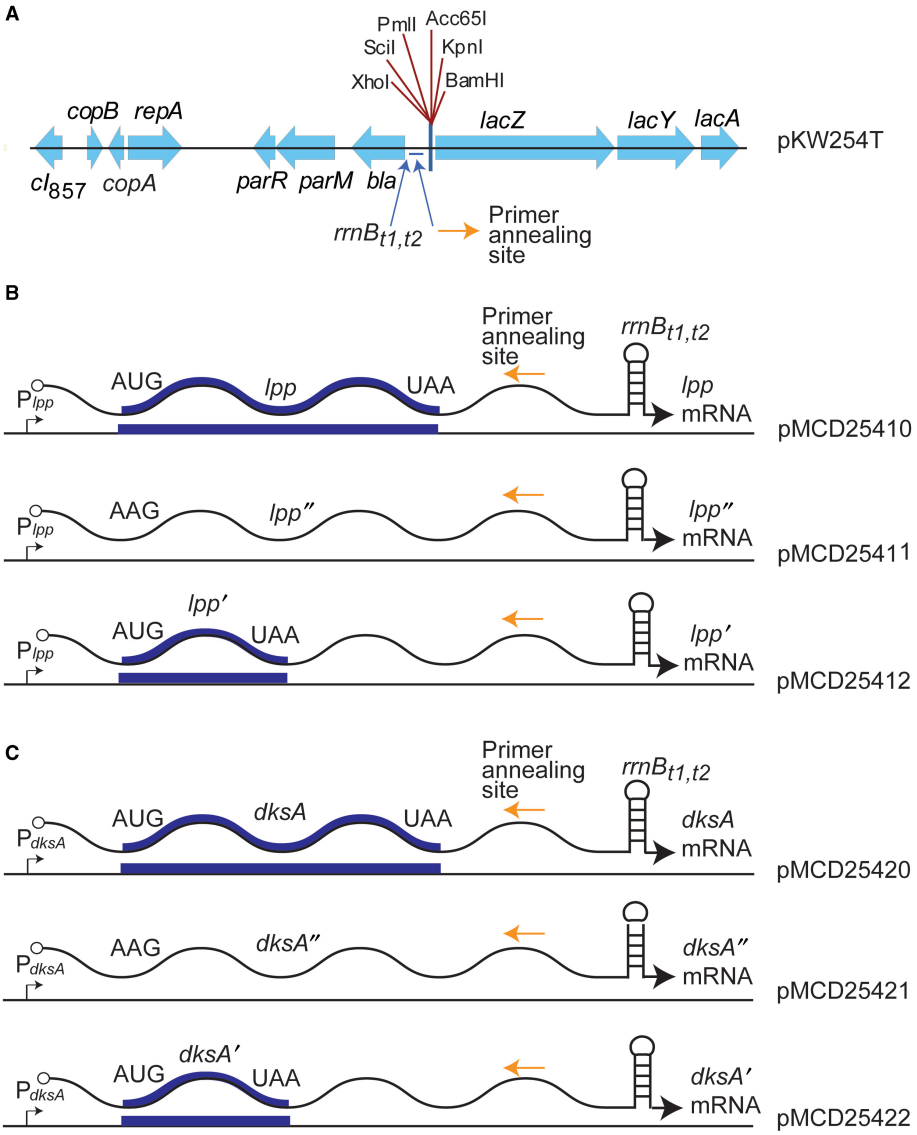

Figure 1. Plasmids used in the analysis of mI activities. (**A**) Plasmid vector used for primer extension analysis of model mRNAs. Plasmid pKW254T is a derivative of an R1 plasmid vector (pOU254) and contains a multiple cloning region with unique restriction sites useful for the insertion of model genes, a primer annealing site and a transcriptional terminator ($rrnB_{t1}$ $rrnB_{t2}$) downstream of the multiple cloning region. The plasmid copy number is temperature amplifiable due to the cI_{857}-controlled λP_R promoter that reads into the replication control region of the plasmid (32). The plasmid was stabilized by the *par* locus of R1 (33). The *lacZYA* genes were not used in this analysis. (**B**) Schematic representation of the genetic content of plasmids used to express wild-type and mutant forms of *lpp* and *dksA* mRNAs. The mRNAs were transcribed from their native promoters but transcription terminated in the $rrnB_{t1}$ $rrnB_{t2}$ terminators of the pKW254T plasmid. Translational start and stop codons are indicated with arrows. Three different variants of the *lpp* gene were inserted into pKW254T. Plasmid pMCD25410 contains the wild-type *lpp* gene; whereas, pMCD25412 carries *lpp* with an extra A base inserted between the fifth and the sixth codons thereby generating a smaller reading frame with a different codon content. The 'frameshifted' mRNA was called *lpp′*. Plasmid pMCD25411 carries *lpp* with the start codon changed from ATG to AAG, thus rendering the RNA non-translatable. This non-translated mRNA was called *lpp″*. (**C**) Plasmid pMCD25420 produces wild-type *dksA* mRNA, pMCD25422 produces *dksA* mRNA with an A base inserted between the second and the third codons (*dksA′* mRNA); whereas, pMCD25421 produces a *dksA* mRNA with the ATG start codon changed to AAG (*dksA″* mRNA). The *lpp* and *dksA* genes shown in (B) and (C) are transcribed from their native promoters.

plasmids shown in Figure 1B and C. Finally, we followed the decay patterns of *lpp* and *dksA* mRNAs after mI induction (Figure 2A and B, respectively). As seen, the levels of the translated, wild-type versions of *lpp* and *dksA* mRNAs decreased rapidly after induction of *relE* and *higB-1*. In contrast, the non-translated versions of the *lpp* and *dksA* mRNAs (denoted *lpp″* and *dksA″* in Figure 2) were much more stable. This result was in agreement with previous analyses showing that RelE and HigB-1 cleave translated RNAs only (15,18). Addition of chloramphenicol, that also inhibits translation rapidly and efficiently, did not mediate decay of any of the model mRNAs (Figure 2, left panels).

Next, we analysed the effect of *yoeB* induction. As seen from Figure 2, *yoeB* induction also destabilized

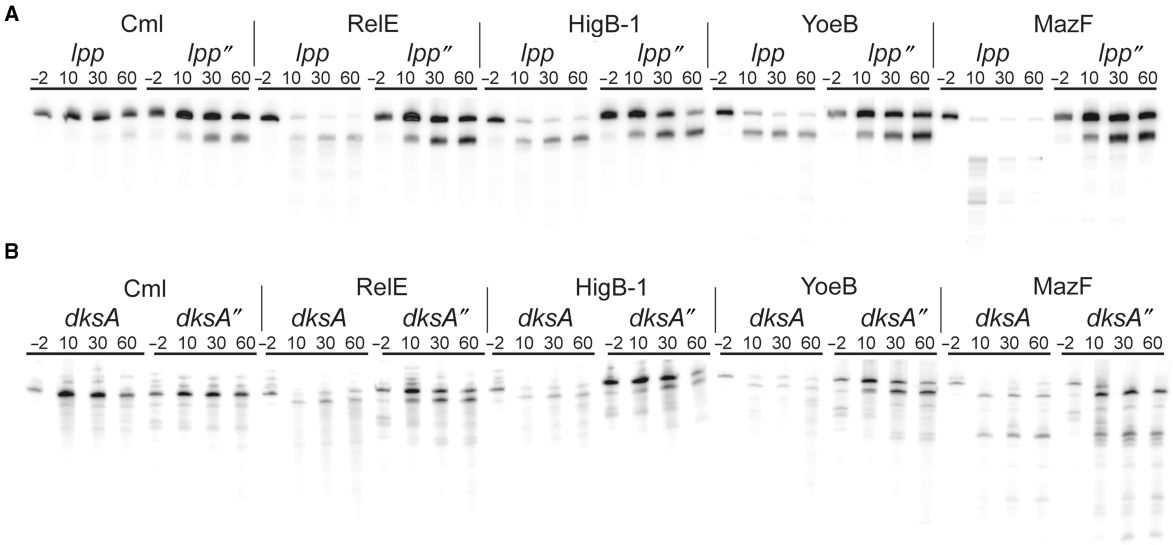

Figure 2. Metabolic stability of *lpp* and *dksA* mRNAs after induction of mI genes. Plasmids pMG3323 (pBAD::*relE*), pMCD3 (pBAD::*higB-1*), pRB100 (pBAD::*yoeB*) and pMCD3326 (pBAD::SD_{opt}::*mazF*) carry the respective mI genes downstream of the arabinose-inducible pBAD promoter. Cells were grown exponentially at 37°C in LB medium. At time 0, translation was inhibited by addition of chloramphenicol (50 μg ml^{-1}) or by addition of arabinose (0.2%) to induce mI gene transcription. (**A**) MG1655Δ*lpp* containing either pSC710 (wild-type *lpp*) or pSC711 (start codon in *lpp* was changed from ATG to AAG; *lpp″*), and one of the mI-expression plasmids. (**B**) MG1655Δ*dksA* containing one of the plasmids, pMCD25420 (wild-type *dksA*) or pMCD25421 (start codon of *dksA* was changed from ATG to AAG; *dksA″*) and one of the mI-expression plasmids. These experiments were accomplished at least three times.

the wild-type *lpp* and and *dksA* mRNAs. Interestingly, however, induction of *yoeB* did not mediate decay of the non-translated versions of the two model mRNAs. This result indicates that YoeB activity depends on translation, as has been shown previously for RelE and HigB-1 (15,18).

Translational reading frame determines the YoeB mRNA cleavage pattern

The above result indicated that YoeB activity *in vivo* requires the substrate RNA to be translated. To investigate YoeB cleavage specificity, we performed primer extension analysis on the wild-type and non-translated versions of *lpp* and *dksA* mRNAs (Figures 3 and 4). We included frameshift variants of *lpp* and *dksA* mRNAs in the analysis (denoted *lpp′* and *dksA′*). For comparison, we included RelE and HigB-1 in the analysis. RelE induced the strongest cleavages in wild-type *lpp* and *dksA* mRNAs, but the cleavage patterns *per se* were similar for all three mIs: in all three cases, the non-translated 5′- and 3′-regions of the mRNAs were not cleaved at all. In contrast, the second codons and the UAA stop codons exhibited strong cleavages in all three cases. All three mRNAs were also cleaved at internal codons usually between the second and the third bases of the codons.

The non-translated *lpp″* and *dksA″* mRNA variants exhibited a strikingly different pattern: the only specific cleavages seen with these model RNAs occurred at the second codon. Most notably, the very strong cleavages seen at the stop codons in the wild-type RNAs were completely absent in the *lpp″* and *dksA″* mRNAs. These results show that the YoeB, RelE and HigB-1 cleavages in the model mRNAs generally required the RNAs to be translated. The cleavages seen at the second codons of *lpp″* and *dksA″* may be a consequence of the presence of strong Shine and Dalgarno sequences upstream of the mutated start codons (AUG was changed to AAG in both *lpp″* and *dksA″*) that can load the non-translated RNAs at the ribosome and thereby position the second codon at the A site. In turn, the second codon will be susceptible to mI cleavage even though translation cannot initiate at the AAG start codon. In all three cases, the *dksA″* mRNA analysis revealed primer extension bands located 21- to 23-nt downstream of the mutated start codon. However, these bands were non-specific because inhibition of translation by the addition of chloramphenicol also induced the formation of these bands (data not shown).

A final proof that YoeB-mediated mRNA cleavage depends on translation came with the analysis of the *lpp′* and *dksA′* frameshift mutants. Both frameshift mutations introduced very similar changes in the YoeB-, RelE- and HigB-1-mediated cleavage patterns: the cleavages in the native stop codons in the wild-type *lpp* and *dksA* mRNAs were abolished (Figures 3B and 4B) concomitantly with the appearance of strong cleavages in the new stop codons in the 'frameshifted' *lpp′* and *dksA′* mRNAs (marked as UAA in Figures 3A and 4A). Moreover, the cleavage patterns seen with the 'frameshifted' mRNAs were in general strikingly different from those of the wild-type mRNAs. As expected, the primer extension bands reflecting cleavages at the second codons of *lpp′* and *dksA′* mRNAs were shifted one base up (as compared to the wild-type RNAs), consistent with the mutational insertion of one base at the 5′-end of the reading frames (Figures 3A and 4A).

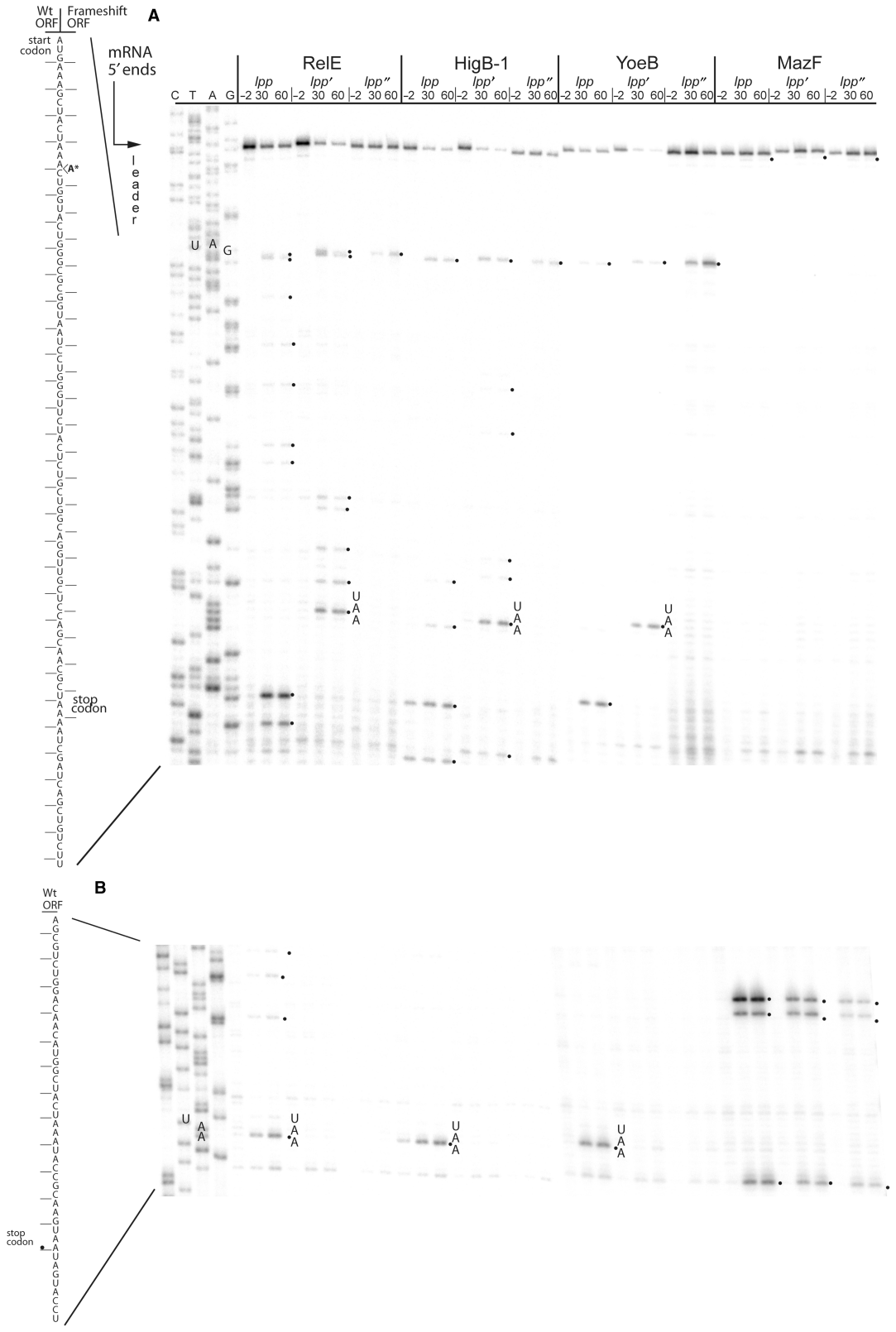

Figure 3. mI-induced cleavage patterns of wild-type and mutated *lpp* mRNAs. The strains MG1655Δ*lpp*/pMCD25410 (wild-type *lpp*), MG1655Δ*lpp*/pMCD25412 (*lpp′*—contains a frameshift mutation in the *lpp* gene) or MG1655Δ*lpp*/pMCD25411 (*lpp″*—the start codon has been changed from ATG to AAG) were co-transformed with the plasmids, pMG3323 (pBAD::*relE*), pMCD3 (pBAD::*higB-1*), pRB100 (pBAD::*yoeB*) and pMCD3326 (pBAD::SDopt::*mazF*). These strains were grown exponentially in LB medium at 37°C and 0.2% arabinose was added at time 0 to induce transcription of the mIs. The Figure shows primer extension reactions. (**A**) The 5′-ends of *lpp* mRNAs were mapped using the primer lpp26. (**B**) The mRNA regions close to the stop codon of *lpp* were mapped using the primer pKW71D-3#PE. Numbers are time points of cell sampling relative to the addition of arabinose. Significant cleavage sites are indicated with black dots. These experiments were accomplished at least three times.

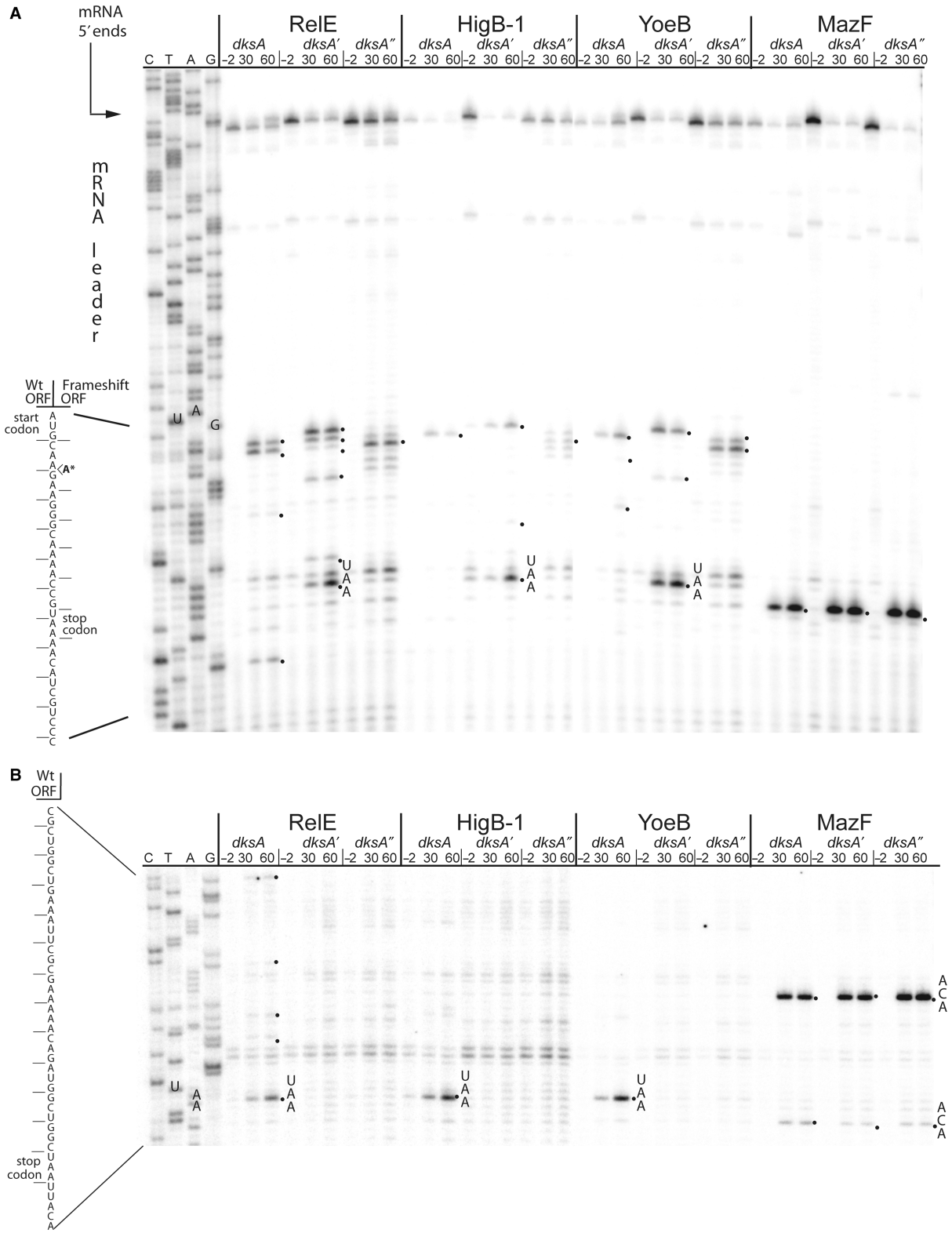

Figure 4. mI-induced cleavage patterns of wild-type and mutated dksA mRNAs. The strains MG1655ΔdksA/pMCD25420 (wild-type *dksA*), MG1655ΔdksA/pMCD25422 (*dksA′*—contains a frameshift mutation in the *dksA* gene) or MG1655ΔdksA/pMCD25421 (*dksA″*—the start codon has been changed from ATG to AAG) were co-transformed with the plasmids, pMG3323 (pBAD::*relE*), pMCD3 (pBAD::*higB-1*), pRB100 (pBAD::*yoeB*) and pMCD3326 (pBAD::SDopt::*mazF*). The strains were grown exponentially in LB medium at 37°C and 0.2% arabinose added at time 0 to induce transcription of the mIs. (**A**) The 5′-ends of the *dksA* mRNAs were mapped using the primer *dksA* PE1. (**B**) The mRNA regions close to the stop codon of *dksA* were mapped using the primer pKW71D-3#PE. Numbers are time points of cell sampling relative to the addition of arabinose. Significant cleavage sites are indicated with black dots. These experiments were accomplished at least three times.

We note that the cleavage patterns mediated by *relE*, *higB-1* and *yoeB* induction were very similar on all six model mRNAs. That all three mIs preferred specific codons rather than specific sequences was further supported by the observation that the cleavage patterns of the wild-type mRNAs were strikingly different from that of the frameshifted mRNAs. Thus, it is the translational reading frame of a given mRNA rather than the sequence itself that determines the cleavage pattern.

In agreement with the northern blotting analyses (Figure 2), our primer extension analyses confirmed that the non-translatable *lpp″* and *dksA″* model mRNAs were more stable than the translated versions of the mRNAs. This conclusion comes from the observation that the amount of full-length mRNA clearly decreased in cases of the translated mRNAs (*lpp*, *lpp′*, *dksA* and *dksA′*); whereas, this was not the case for the non-translated versions (*lpp″* and *dksA″*) (see arrows pointing at mRNA 5′-ends in Figures 3A and 4A). Again, the YoeB-mediated mRNA cleavage patterns were very similar to those mediated by RelE and HigB-1.

Previously, tmRNA was used as a model substrate in the analysis of mI activity (15). Thus, RelE cleaves within the reading frame of wt tmRNA; whereas, RelE did not cleave a non-translated version of tmRNA. To compare our results with these earlier observations, we decided to investigate how expression of HigB-1 and YoeB affects the wild-type and the non-translated version of tmRNA (resume codon GCA was changed to UAA). As seen from Figure 5, RelE, HigB-1 and YoeB cleaved the translated but not the non-translated version of tmRNA, and tmRNA cleavage was confined to its coding region. These results support the conclusion that HigB-1 and YoeB cleavage depends on translation.

MazF exhibits translation-dependent and -independent mRNA cleavage

It has not been resolved whether MazF cleavage of mRNA *in vivo* depends on translation. To address this question, we first compared the decay patterns of wild-type and non-translated *lpp* and *dksA* mRNAs after induction of *mazF*. As seen from Figure 2A, the amount of wild-type *lpp* mRNA decreased rapidly after *mazF* induction. However, as with the RelE family of mIs, the non-translated *lpp* mRNA was not affected by MazF expression. In contrast, the translated and non-translated versions of the *dksA* mRNA were both very rapidly cleaved by MazF (Figure 2B).

Translation affects MazF cleavage efficiency but not cleavage specificity

Next, we employed primer extension analyses to investigate how translation affects MazF-induced mRNA cleavage. It has previously been reported that MazF cleaves specifically at ACA sites, independently of translation (14). Consistently, induction of MazF mediated cleavage at two ACA sites located upstream of the stop codon of *lpp* (Figure 3B). The *lpp* mRNA contains one additional ACA site at its very 5′-end. As seen, MazF also cleaved this ACA site (Figure 3A). Thus, all ACA sites in *lpp* mRNA were cleaved by MazF, independently of their location in the RNA. MazF also mediated cleavage at an ACC site just downstream of the stop codon of *lpp* mRNA (Figure 3B), suggesting that MazF cleavage is not absolutely restricted to ACA sites.

We then performed primer extension analysis on the frameshifted and non-translated versions of *lpp* mRNA after induction of *mazF*. Strikingly, abolition of translation did not change the MazF-mediated cleavage pattern *per se* (Figure 3). However, the efficiency of cleavage was significantly reduced in the 3′-end of the *lpp′* mRNA variant as compared to the wild-type (Figure 3B). Cleavage of the *lpp″* mRNA was even more reduced, consistent with the high degree of stability of the full-length *lpp″* mRNA observed by northern blotting analysis (Figure 2A). In contrast, the strengths of the cleavages at the 5′ ACA sites of the three *lpp* mRNA variants were very similar (Figure 3A, top).

The *dksA* mRNA has three ACA sites, one located seven codons downstream of the start codon, one four codons upstream of the stop codon and one just downstream of the stop codon. Ectopic induction of *mazF* mediated cleavage at all three sites in the wild-type *dksA* mRNA (Figure 4). Moreover, the *dksA′* and *dksA″* variant mRNAs were cleaved in a pattern that was indistinguishable from that of the wild-type mRNA. Thus, translation does not affect MazF cleavage of the *dksA* mRNA.

For completion, we included tmRNA in our analysis of MazF-mediated RNA cleavage (Figure 5) even though tmRNA is devoid of *bona fide* MazF cleavage sites (5′-ACA-3′). Unexpectedly, we observed a weak MazF-mediated cleavage in an ACU site in the coding region of tmRNA that occurred in both the translated and non-translated forms of the RNA. This was unexpected since MazF has been shown to be highly specific for ACA sites. One possible explanation for this observation is that MazF in this particular case had a relaxed cleavage site specificity. Another, more likely explanation, is that the tmRNA cleavage was a secondary effect caused by the MazF-mediated global inhibition of translation.

DISCUSSION

Here, we developed a rapid and straightforward method to analyse mI activity on two model mRNAs. The coverage of the 3′-region of a given reading frame by primer extension analysis requires that a primer can anneal to the non-translated mRNA 3′-end. Many bacterial 3′-ends are short and fold into stable secondary structures (such as Rho-independent transcriptional terminators) that may prevent efficient annealing of a DNA primer used in the primer extension analysis. To circumvent this problem, we constructed a low copy number plasmid (pKW254T) carrying a primer annealing site flanked by a multiple cloning region at the 5′-side and a transcriptional terminator at the 3′-side (Figure 1A). Using this plasmid, we were able to analyse the entire reading frames of two model mRNAs. This experimental set-up should be generally useful for the *in vivo* analysis of mIs.

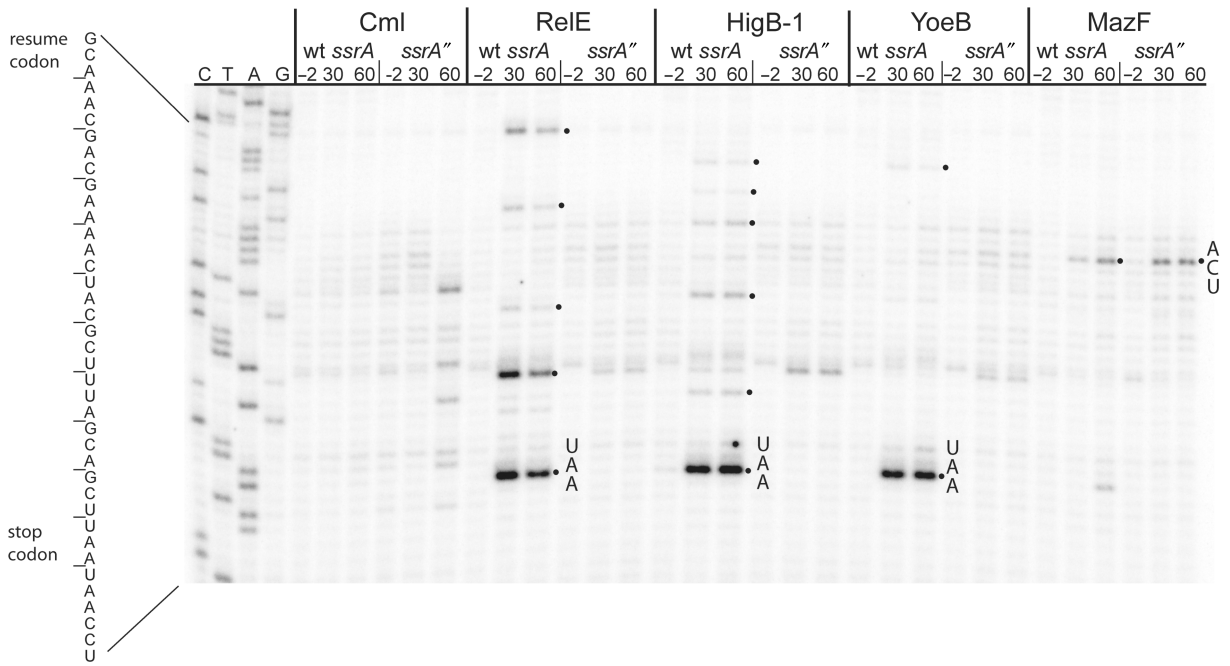

Figure 5. Primer extension analysis of wild-type and mutated tmRNA before and after mI induction. Strains MG1655Δ*ssrA*/pSC320 (wt *ssrA*) and MG1655Δ*ssrA*/pSC321 (*ssrA″*—the resume codon of tmRNA was changed from GCA to TAA) also carrying one of the plasmids pMG3323 (pBAD::*relE*), pMCD3 (pBAD::*higB-1*), pRB100 (pBAD::*yoeB*) or pMCD3326 (pBAD::SD_{opt}::*mazF*) were grown exponentially at 37°C. At time 0, translation was inhibited by the addition of 50 μg ml^{-1} chloramphenicol or by induction of mI transcription with 0.2% arabinose. Numbers are time points of cell sampling relative to the addition of arabinose. Significant cleavage sites are indicated with black dots. The RNA was mapped using the primer 10SA-2. This experiment was performed at least three times.

Two conclusions can be drawn from the analyses presented here. First, YoeB-induced mRNA cleavage *in vivo* required that the mRNA is translated and cleavage occurs only within translated regions of the RNA (Figures 3–5). This requirement was very similar to that exhibited by RelE from *E. coli* and RelE homologues from *V. cholerae* (HigB-1 and -2) and Archaea (14,15,18,30). In contrast, YoeB was able to cleave naked RNA *in vitro*, independent of the presence of ribosomes (21). We can only speculate about the reason for this observation. A remote possibility that we could not exclude was that the mRNA cleavages seen after ectopic production of YoeB *in vivo* was caused by fortuitous induction of a chromosome-encoded mI whose activity depends on translation. To rule out this possibility, we repeated the experiments shown in Figures 3–5 in an *E. coli* K-12 strain devoid of the three known *relBE* homologues and the two known *mazEF* homologues (data not shown). RNAs prepared from the multiple deletion strain exhibited YoeB-mediated cleavage patterns indistinguishable of those seen with RNA from the wild-type strain (MG1655Δlpp) (data not shown). A more likely explanation invokes that YoeB has a high affinity for RNA substrates presented at the ribosomal A site and that the presumed few YoeB molecules that are required to inhibit translation are titrated by the ribosomes. In turn, such titration would prevent random cleavage of cellular RNAs.

The second conclusion was that MazF cleavage specificity did not depend on translation. Previously, we observed that a non-translated version of *lpp* mRNA was cleaved much slower than the isogenic wild-type mRNA (5). This observation was seemingly at variance with the *in vitro* activity of MazF (14,23). However, our new analyses can now explain the discrepancy. We observed that MazF cleaved at ACA sites in both *lpp* and *dksA* mRNAs. The three versions of *dksA* mRNA were cleaved with equal efficiencies, thus ruling out that translation plays any role of the reaction in this case (Figure 4). In contrast, the cleavages in *lpp* mRNA were much weaker in the non-translated *lpp′* mRNA than in the wild-type mRNA (Figures 2 and 3). The *lpp′* mRNA carrying the frameshift mutation exhibited an intermediary susceptibility to MazF cleavage (Figure 3). These results show that MazF cleavage does not strictly depend on translation, that is, MazF cleavage occurs whether or not the substrate mRNA is translated. However, translation enhanced MazF-mediated *lpp* cleavage. The most likely explanation for this observation is that ribosomes translating the target mRNA disrupts secondary structure that is inhibitory to cleavage by MazF that prefers single-stranded RNA substrates (23). A recent analysis of two MazF homologues supports this interpretation (24). These authors showed that addition of CspA, the major cold-shock protein of *E. coli* that prevent the formation of secondary structures in RNA (31), stimulated MazF homologue cleavage at target sites predicted to be folded into RNA secondary structure. These results are consistent with the proposal that the ACA sites in *lpp* mRNA are shielded by secondary structure and the ribosomes disrupt these interactions during translation.

The translation-independent MazF cleavage of *dksA* mRNA indicated that the ACA sites in this case was present in single-stranded configurations.

The biological function of most TA loci is still unknown. However, the observations presented here show that mIs have very different requirements for mRNA target cleavage, thus raising the possibility that *relBE* and *mazEF* loci play different biological roles.

ACKNOWLEDGEMENT

We thank K. Winther for the construction of pKW254T and Bhaskar Chandra Mohan Ramisetty for the construction of pRB100. This work was supported by the Centre for mRNP Biogenesis and Metabolism of the Danish National Research Foundation and the WELCOME TRUST.

FUNDING

Centre for mRNP Biogenesis and Metabolism sponsored by the Danish Research Foundation.

Conflict of interest statement. None declared.

REFERENCES

1. Gerdes,K., Christensen,S.K. and Lobner-Olesen,A. (2005) Prokaryotic toxin-antitoxin stress response loci. *Nat. Rev. Microbiol.*, **3**, 371–382.
2. Inouye,M. (2006) The discovery of mRNA interferases: implication in bacterial physiology and application to biotechnology. *J. Cell. Physiol.*, **209**, 670–676.
3. Pandey,D.P. and Gerdes,K. (2005) Toxin - antitoxin loci are highly abundant in free-living but lost from host-associated prokaryotes. *Nucleic Acids Res.*, **33**, 966–976.
4. Christensen,S.K., Mikkelsen,M., Pedersen,K. and Gerdes,K. (2001) RelE, a global inhibitor of translation, is activated during nutritional stress. *Proc. Natl Acad. Sci. USA*, **98**, 14328–14333.
5. Christensen,S.K., Pedersen,K., Hansen,F.G. and Gerdes,K. (2003) Toxin-antitoxin loci as stress-response-elements: ChpAK/MazF and ChpBK cleave translated RNAs and are counteracted by tmRNA. *J. Mol. Biol.*, **332**, 809–819.
6. Gerdes,K. (2000) Toxin-antitoxin modules may regulate synthesis of macromolecules during nutritional stress. *J. Bacteriol.*, **182**, 561–572.
7. Gvakharia,B.O., Permina,E.A., Gelfand,M.S., Bottomley,P.J., Sayavedra-Soto,L.A. and Arp,D.J. (2007) Global transcriptional response of nitrosomonas europaea to chloroform and chloromethane. *Appl. Environ. Microbiol.*, **73**, 3440–3445.
8. Tachdjian,S. and Kelly,R.M. (2006) Dynamic metabolic adjustments and genome plasticity are implicated in the heat shock response of the extremely thermoacidophilic archaeon Sulfolobus solfataricus. *J. Bacteriol.*, **188**, 4553–4559.
9. Park,S. and Ely,R.L. (2008) Genome-wide transcriptional responses of Nitrosomonas europaea to zinc. *Arch. Microbiol.*, **189**, 541–548.
10. Fu,Z., Donegan,N.P., Memmi,G. and Cheung,A.L. (2007) Characterization of MazFSa, an endoribonuclease from Staphylococcus aureus. *J. Bacteriol.*, **189**, 8871–8879.
11. Buts,L., Lah,J., Dao-Thi,M.H., Wyns,L. and Loris,R. (2005) Toxin-antitoxin modules as bacterial metabolic stress managers. *Trends Biochem. Sci.*, **30**, 672–679.
12. Liu,M., Zhang,Y., Inouye,M. and Woychik,N.A. (2008) Bacterial addiction module toxin Doc inhibits translation elongation through its association with the 30S ribosomal subunit. *Proc. Natl Acad. Sci. USA*, **105**, 5885–5890.
13. Pedersen,K., Zavialov,A.V., Pavlov,M.Y., Elf,J., Gerdes,K. and Ehrenberg,M. (2003) The bacterial toxin RelE displays codon-specific cleavage of mRNAs in the ribosomal A site. *Cell*, **112**, 131–140.
14. Zhang,Y., Zhang,J., Hoeflich,K.P., Ikura,M., Qing,G. and Inouye,M. (2003) MazF cleaves cellular mRNAs specifically at ACA to block protein synthesis in Escherichia coli. *Mol. Cell*, **12**, 913–923.
15. Christensen,S.K. and Gerdes,K. (2003) RelE toxins from bacteria and Archaea cleave mRNAs on translating ribosomes, which are rescued by tmRNA. *Mol. Microbiol.*, **48**, 1389–1400.
16. Anantharaman,V. and Aravind,L. (2003) New connections in the prokaryotic toxin-antitoxin network: relationship with the eukaryotic nonsense-mediated RNA decay system. *Genome Biol.*, **4**, R81.
17. Budde,P.P., Davis,B.M., Yuan,J. and Waldor,M.K. (2007) Characterization of a higBA toxin-antitoxin locus in Vibrio cholerae. *J. Bacteriol.*, **189**, 491–500.
18. Christensen-Dalsgaard,M. and Gerdes,K. (2006) Two higBA loci in the Vibrio cholerae superintegron encode mRNA cleaving enzymes and can stabilize plasmids. *Mol. Microbiol.*, **62**, 397–411.
19. Motiejunaite,R., Armalyte,J., Markuckas,A. and Suziedeliene,E. (2007) Escherichia coli dinJ-yafQ genes act as a toxin-antitoxin module. *FEMS Microbiol. Lett.*, **268**, 112–119.
20. Schmidt,O., Schuenemann,V.J., Hand,N.J., Silhavy,T.J., Martin,J., Lupas,A.N. and Djuranovic,S. (2007) prlF and yhaV encode a new toxin-antitoxin system in Escherichia coli. *J. Mol. Biol.*, **372**, 894–905.
21. Kamada,K. and Hanaoka,F. (2005) Conformational change in the catalytic site of the ribonuclease YoeB toxin by YefM antitoxin. *Mol. Cell*, **19**, 497–509.
22. Zhang,Y., Zhang,J., Hara,H., Kato,I. and Inouye,M. (2005) Insights into the mRNA cleavage mechanism by MazF, an mRNA interferase. *J. Biol. Chem.*, **280**, 3143–3150.
23. Zhang,J., Zhang,Y., Zhu,L., Suzuki,M. and Inouye,M. (2004) Interference of mRNA function by sequence-specific endoribonuclease PemK. *J. Biol. Chem.*, **279**, 20678–20684.
24. Zhu,L., Phadtare,S., Nariya,H., Ouyang,M., Husson,R.N. and Inouye,M. (2008) The mRNA interferases, MazF-mt3 and MazF-mt7 from Mycobacterium tuberculosis target unique pentad sequences in single-stranded RNA. *Mol. Microbiol.*, **69**, 559–69.
25. Munoz-Gomez,A.J., Santos-Sierra,S., Berzal-Herranz,A., Lemonnier,M. and az-Orejas,R. (2004) Insights into the specificity of RNA cleavage by the Escherichia coli MazF toxin. *FEBS Lett.*, **567**, 316–320.
26. Munoz-Gomez,A.J., Lemonnier,M., Santos-Sierra,S., Berzal-Herranz,A. and az-Orejas,R. (2005) RNase/anti-RNase activities of the bacterial parD toxin-antitoxin system. *J. Bacteriol.*, **187**, 3151–3157.
27. Nariya,H. and Inouye,M. (2008) MazF, an mRNA interferase, mediates programmed cell death during multicellular Myxococcus development. *Cell*, **132**, 55–66.
28. Franch,T., Gultyaev,A.P. and Gerdes,K. (1997) Programmed cell death by hok/sok of plasmid R1: processing at the hok mRNA 3′-end triggers structural rearrangements that allow translation and antisense RNA binding. *J. Mol. Biol.*, **273**, 38–51.
29. Guzman,L.M., Belin,D., Carson,M.J. and Beckwith,J. (1995) Tight regulation, modulation, and high-level expression by vectors containing the arabinose PBAD promoter. *J. Bacteriol.*, **177**, 4121–4130.
30. Christensen,S.K., Maenhaut-Michel,G., Mine,N., Gottesman,S., Gerdes,K. and Van,M.L. (2004) Overproduction of the Lon protease triggers inhibition of translation in Escherichia coli: involvement of the yefM-yoeB toxin-antitoxin system. *Mol. Microbiol.*, **51**, 1705–1717.
31. Jiang,W., Hou,Y. and Inouye,M. (1997) CspA, the major cold-shock protein of Escherichia coli, is an RNA chaperone. *J. Biol. Chem.*, **272**, 196–202.
32. Larsen,J.E., Gerdes,K., Light,J. and Molin,S. (1984) Low-copy-number plasmid-cloning vectors amplifiable by derepression of an inserted foreign promoter. *Gene*, **28**, 45–54.
33. Gerdes,K., Larsen,J.E. and Molin,S. (1985) Stable inheritance of plasmid R1 requires two different loci. *J. Bacteriol.*, **161**, 292–298.